Free-Field (Elastic or Poroelastic) Half-Space Zero-Stress or Related Boundary Conditions

Vincent W Lee [1] and Jianwen Liang [2]

[1] *Professor, Civil & Environmental Engineering, Univ. of Southern California, Los Angeles, CA 90089 USA, vlee@usc.edu*

[2] *Professor, School of Civil Engineering, Tianjin University, Tianjin 300072, China, liang@tju.edu.cn*

ABSTRACT :

The boundary-valued problem for solving for waves scattered and diffracted from surface and sub-surface topographies have attracted much attention to earthquake and structural engineers and strong-motion seismologists since the last century. It is of importance in the design, construction and analysis of earthquake resistant surface and sub-surface structures in seismic active areas that are vulnerable to near field or far field strong-motion earthquakes. The half-space medium can be elastic, or poroelastic and fluid saturated, the later case has attracted much new research in recent years.

The presence of a surface or sub-surface topography, like the case of a surface canyon, valley, canal or structural foundations, or an underground cavity, tunnel or pipe, will result in scattered and diffracted waves being generated. Combined with the free-field input waves, they will together satisfy the appropriate stress and/or displacement boundary conditions at the surface of the topography present in the model. For those problems where analytical solutions are preferred in the studies, this often involves a topography that is either: circular, elliptic, spherical or parabolic in shape. This is because in those coordinate systems, the scattered waves are expressible in terms of orthogonal wave functions, and the surface of the topography often allows the orthogonal boundary conditions to be applied, so that the wave coefficients can be analytically defined.

However, the presence of the half-space boundary makes the problem much more complicated. The scattered wave functions are no longer orthogonal on the flat half-space surface, and the zero-stress or related boundary conditions are no longer simple nor straight forward to apply. This paper will examine the available numerical and approximate methods that have been attempted or proposed, and the direction all future research is taking us to solve this part of the problem.

KEYWORDS: Diffraction, Free-Field, Half-Space, Elastic, Poroelastic

1. INTRODUCTION

Large topographies at half-space surfaces, like, canyons, valleys, canals and structural foundations, large, underground sub-surfaced structures like cavities, pipes, subways or tunnels, are always present in metropolitan areas associated with infrastructure developments in cites. As a result of excitation by incoming seismic waves, their presence will often generate additional waves from diffraction and scattering, resulting amplifications and de-amplification of the input waves, which will affect the deformations, distributions and concentrations of stresses on nearby ground surfaces and the structures on them. It is thus important to fully understand the theoretical and engineering aspects of the effects of such diffraction.

This calls for a need for accurate, analytical method to be developed to study the in-plane responses of buried topographies to input waves. In general, for any wave propagation boundary valued problems, it is necessary to select the right coordinate systems that will allow the vector wave equations of the elastic waves to be separable into scalar wave equations for the P- and SV- wave potentials. However, because of the complexity of the problem involved, simple analytic solutions to diffraction problems by these underground topographies, are limited in both quantities and qualities. For the case of finite topographies in a finite region, like that of

machines, airplanes or space structures like satellites, these would be wave boundary valued problems that can be solved by a finite element program, many versions of which are widely available in industry. For the cases of problems involving infinite or semi-infinite medium, like the case of all half-space wave propagation problems, these finite element software will not be directly applicable. A special "large" finite element may have to be defined to simulate the semi-infinite medium. This will not always be satisfactory.

This is not a new problem. Solving for the scattered wave potentials that need to satisfy the zero-stress boundary conditions at the half-space surface is a classical boundary-valued problem that interested scientists, seismologists and engineers, in particular earthquake engineers, since the turn of the 20th Century. The zero-stress boundary conditions at the surface of the half space in the presence of surface and sub-surface topographies for in-plane cylindrical P- and SV- waves have always been a challenging problems. Unlike the out-of-plane SH waves, the imaging method cannot be applied to in-plane waves. The outgoing cylindrical P- and SV-waves are composed of Hankel functions of radial distance coupled with the sine and cosine functions of angle. Together at the half-space surface the P- and SV- waves functions are not orthogonal over the semi-infinite radial distance from 0 to infinity.

For them to simultaneously satisfy the zero in-plane normal and shear stresses, sophisticated analytic and numerical methods will have to be developed. This paper will consider the various few techniques that can be and have been used to tackle this boundary-valued problem.

The free-stress boundary conditions at the half-space surface to be solved here are indeed the most complicated boundary conditions to be satisfied in the present problem. Analytical methods would require all the complicated boundary conditions to be imposed and satisfied simultaneously.

Over the years, numerical approximation to the geometry is often made. This is the case where the flat half-space surface is replaced by a circular surface of large radius, the so-called "large circle approximation" to the half-space surface.

Here, a known existing analytical formulation of the boundary-valued problem is presented, where the Hankel wave functions are expressed in integral forms, changing from cylindrical to rectangular coordinates, when the zero-stress boundary conditions at the half-space surface can be applied in a more straight forward sense. This is the so-called "Fourier Transform Method" for solving the boundary-valued problem.

It is sometimes desired to produce an alternate, simpler approximate estimate of the solution to the boundary-valued problem without going at great lengths to have all the boundary conditions satisfied. It is thus interesting to see what the solution would be like if the half-space boundary conditions are not to be imposed and not to be satisfied, in other words, if they are to be "relaxed". This is the so-called method of "Relaxing the half-space free-stress boundary conditions"

The present method to be introduced may also serve as a general method for more complicated wave propagation problems, like the diffraction problems involving surface and sub-surface topographies in a poroelastic half-space medium.

2. THE MODEL: INCIDENT PLANE P WAVES

As an example to illustrate the method, consider here (Figure 1) the work of Lin et al (2008) of the diffraction of an underground circular tunnel. The following is a summary of the equations The model is a flat half-space medium with a circular region of a tunnel of outer radius 'a' and inner radius 'b' made up of another elastic medium. The half-space is supposed to be elastic, isotropic and homogeneous with mass density ρ and Lamé elastic constants λ, μ. The tunnel is supposed to be elastic with mass density ρ_1 and Lamé elastic constants λ_1, μ_1.

The excitation consists of incident plane P-waves are assumed to have an angle of incidence γ_α with respect to the y-axis, frequency ω and wave number $k_\alpha = \omega / c_\alpha$, where c_α is the P-wave speed. The presence of the half-space flat ground surface will result in both reflected, plane P- & SV- waves. . They are given by the potential function ϕ^i, ϕ^r and ψ^r respectively. The total Free-field P- and SV-waves potentials are the sum of incident and reflected plane waves that satisfy the zero-stress flat ground surface boundary conditions, respectively ϕ^{ff} and ψ^{ff} , are given by, with respect to the (r_1, θ_1) coordinate system (Lin et al, 2008):

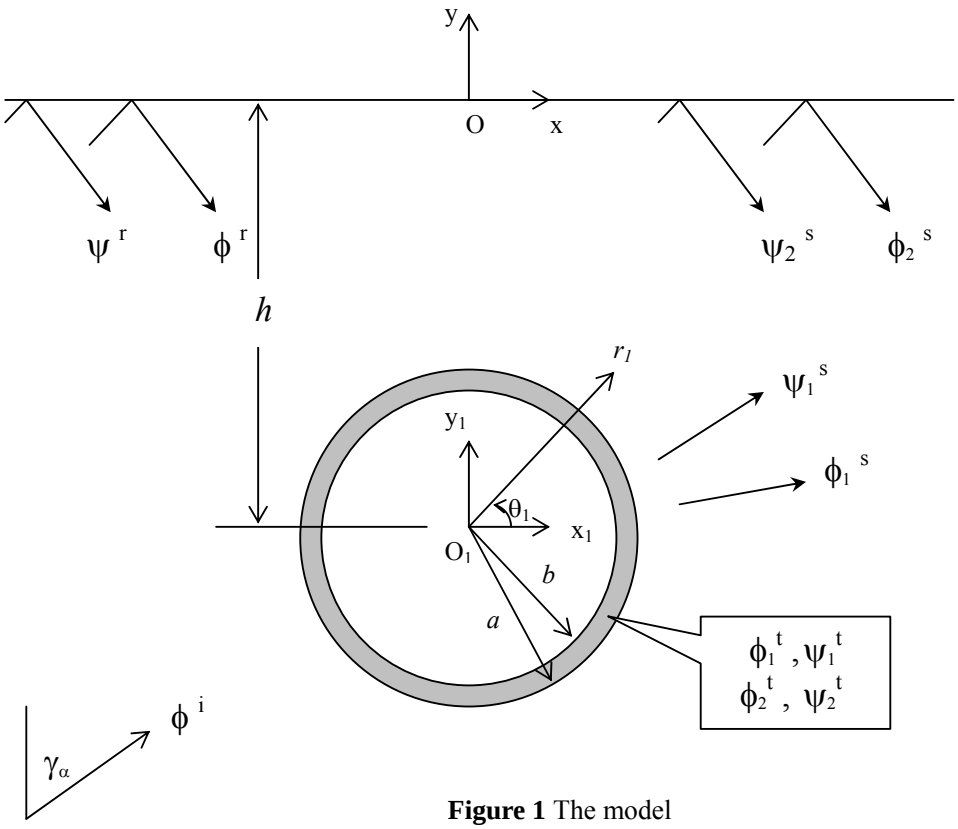

Figure 1 The model

$$\phi^{ff} = \phi^i + \phi^r = \sum_{n=-\infty}^{\infty} a_n J_n(k_\alpha r_1) e^{in\theta_1} \qquad \psi^{ff} = \psi^r = \sum_{n=-\infty}^{\infty} b_n J_n(k_\beta r_1) e^{in\theta_1} \tag{1}$$

where $a_n, b_n, n = 0,1,2,\ldots$ are known coefficients.

The presence of the underground tunnel will result in scattered P- and SV- waves in the half-space. They are represented by Hankel functions of the first kind which represent outgoing cylindrical waves. The P- and SV- scattered potentials, measured with respect to the (r_1, θ_1) coordinates, take the form:

$$\phi_1^s = \sum_{n=-\infty}^{\infty} A_{1,n} H_n^{(1)}(k_\alpha r_1) e^{in\theta_1} \qquad \psi_1^s = \sum_{n=-\infty}^{\infty} B_{1,n} H_n^{(1)}(k_\beta r_1) e^{in\theta_1} \tag{2}$$

The presence of the half-space surface will result in additional P- SV- waves reflected into the half-space, of the form, with respect to the (r_1, θ_1) coordinates, which are finite everywhere:

$$\phi_2^s = \sum_{n=-\infty}^{\infty} A_{2,n} J_n(k_\alpha r_1) e^{in\theta_1} \qquad \psi_2^s = \sum_{n=-\infty}^{\infty} B_{2,n} J_n(k_\beta r_1) e^{in\theta_1} \tag{3}$$

The Total Scattered and Reflected Waves in the Half-Space in cylindrical coordinates are given by, from equations (1), (2) and (3):

$$\begin{aligned} \phi &= \phi^{ff} + \phi_1^s + \phi_2^s = \sum_{n=-\infty}^{\infty} \left[\left(a_n + A_{2,n} \right) J_n(k_\alpha r_1) + A_{1,n} H_n^{(1)}(k_\alpha r_1) \right] e^{in\theta_1} \\ \psi &= \psi^{ff} + \psi_1^s + \psi_2^s = \sum_{n=-\infty}^{\infty} \left[\left(b_n + B_{2,n} \right) J_n(k_\beta r_1) + B_{1,n} H_n^{(1)}(k_\beta r_1) \right] e^{in\theta_1} \end{aligned} \tag{4}$$

The region within the tunnel is $b \le r \le a,\ 0 \le \theta \le 2\pi$, with the outer circular surface at $r = a$ in contact with the half-space medium and the inner circular surface $r = b$, the surface of the inner cavity of the tunnel. The presence of two circular surfaces will result in both outgoing and incoming cylindrical waves, the total transmitted waves inside the tunnel as:

$$\begin{aligned} \phi^t &= \phi_1^t + \phi_2^t = \sum_{n=-\infty}^{\infty} \left(C_{1,n} H_n^{(1)}(k_\alpha r_1) + C_{2,n} H_n^{(2)}(k_\alpha r_1) \right) e^{in\theta_1} \\ \psi^t &= \psi_1^t + \psi_2^t = \sum_{n=-\infty}^{\infty} \left(D_{1,n} H_n^{(1)}(k_\beta r_1) + D_{2,n} H_n^{(2)}(k_\beta r_1) \right) e^{in\theta_1} \end{aligned} \tag{5}$$

3. THE BOUNDARY CONDITIONS AND SOLUTIONS

The complete solution of this boundary-valued problem would consist of the boundary conditions:

i) Zero-Stress at the Tunnel Inner Cavity Surface (r = b)
ii) Stress & Displacement Continuity at the Tunnel Outer Surface, and
iii) Zero-Stress at the Half-Space Surface (y = 0).

The first two sets of boundary conditions are on circular surfaces in cylindrical coordinates, while the last set is on the flat surface in rectangular coordinates. For cylindrical waves, the boundary conditions i) and ii) are thus much more trivial to apply. The readers are referred to Lin et al (2008) for their detailed equations. We will concentrate in this paper only on the discussion of the zero-stress boundary conditions.

Almost 20 years ago, an approximation to the flat surface is proposed. Lee and Cao (1989), Cao and Lee (1990) used a large circular, almost flat surface to approximate the half-space surface and presented numerical solutions to diffraction problems of surface circular canyons of various depths by incident plane P- and SV- waves. Todorovska and Lee (1990, 1991a,b) solved by the same method for anti-plane SH waves and incident Rayleigh waves on circular canyons. Later, Lee and Karl (1993a,b) extended the method to diffraction of P-, SV- waves for diffraction by circular underground cavities. Also Lee and Wu (1994a,b) used the same method of approximations for arbitrary-shaped two-dimensional canyons. Finally, Davis et al (2001) used such an approximate method in their case studies of the failure of underground pipes. Recently, Liang et al (2000, 2001a,b, 2002, 2003, 2004a,b,c) continued the analyses by the same method from problems for circular-arc canyons and valleys, underground pipes to that of the poroelastic half-space.

Currently in these last few years, the above method was met with severe criticism. It was felt that the large circular approximation does not reduce to the flat half-space when the radius, *R*, of the circular surface approaches infinity, because as $R \to \infty$, the Bessel functions used in the transformation would approach zero. It was felt that without a method to satisfactorily satisfy the free-stress boundary conditions at the half-space surface, one would prefer rather to relax the free-stress conditions than to use the large circle approximations (Todorovska and Yousef, 2006; Liang et al, 2006).

With respect to the $\{x, y\}$ coordinates with origin at *O* at the half-space surface, the zero-stress boundary conditions at the half-space surface are to be applied only to the scattered P- and SV-wave potentials. $\phi_1^s + \phi_2^s$

and $\psi_1^s + \psi_2^s$. They are represented in cylindrical (polar) coordinates, and the above zero-stress conditions are to be applied at the flat surface $y = 0$ given in rectangular coordinates. As stated at the introduction, applying such equations at the flat half-space surface to cylindrical waves is not a trivial matter, and previous attempt has been made to approximate the flat boundary surface by a large circular surface. The following approach is to leave the half-space surface flat and to follow the approach of Lamb's problem (1904) to represent each mode or term of the Hankel wave series as an integral in rectangular coordinates. In other words, the Fourier transform of the wave functions is taken. Take the case of the n^{th} mode of the P- and SV-wave scattered potentials:

$$\begin{aligned} H_n^{(1)}(k_\alpha r_1)e^{in\theta_1} &= \int_{-\infty}^{\infty}\left[(\frac{i^{-n}}{i\pi\nu_\alpha})(\frac{k-\nu_\alpha}{k_\alpha})^n\right] e^{ikx_1-\nu_\alpha|y_1|}\, dk \\ H_n^{(1)}(k_\beta r_1)e^{in\theta_1} &= \int_{-\infty}^{\infty}\left[(\frac{i^{-n}}{i\pi\nu_\beta})(\frac{k-\nu_\beta}{k_\beta})^n\right] e^{ikx_1-\nu_\beta|y_1|}\, dk \end{aligned} \tag{6}$$

where $\nu_\alpha = \sqrt{k^2 - k_\alpha^2}$, and $\nu_\beta = \sqrt{k^2 - k_\beta^2}$. The case of $n = 0$ in the above integral expressions was first used by Lamb (1904) in his paper on the tremors. Here in Equation (7), the Hankel wave functions in the $\{r_1, \theta_1\}$ cylindrical coordinates are transformed to the $\{x_1, y_1\}$ rectangular coordinates suitable for the zero-stress boundary conditions at the flat half-space surface. Each integrand in the above integrals is the Fourier Transform of the n^{th} mode of the wave function.

Using the $\{x, y\}$–coordinate with origin at O on the half-space surface, the integral takes the form, with $y_1 = y + h$, in the region $0 \le y_1 \le h$, or $-h \le y \le 0$, apply now the transform to the whole set of terms for the P- and SV- potentials:

$$\begin{aligned} \phi_1^s = \phi_1^s(r_1,\theta_1) = \sum_{n=-\infty}^{\infty} A_{1,n}H_n^{(1)}(k_\alpha r_1)e^{in\theta_1} = \phi_1^s(x,y) = \int_{-\infty}^{\infty} [\mathbf{a_1}(k)]e^{ikx-\nu_\alpha|y|}dk \\ \psi_1^s = \psi_1^s(r_1,\theta_1) = \sum_{n=-\infty}^{\infty} B_{1,n}H_n^{(1)}(k_\beta r_1)e^{in\theta_1} = \psi_1^s(x,y) = \int_{-\infty}^{\infty} [\mathbf{b_1}(k)]e^{ikx-\nu_\beta|y|}dk \end{aligned} \tag{7}$$

such that

$$\begin{Bmatrix} \mathbf{a_1}(k) \\ \mathbf{b_1}(k) \end{Bmatrix} = \sum_{n=-\infty}^{\infty} \frac{i^{-n}}{i\pi} \begin{bmatrix} \zeta_{\alpha,n}(h)/\nu_\alpha & 0 \\ 0 & \zeta_{\beta,n}(h)/\nu_\beta \end{bmatrix} \begin{Bmatrix} A_{1,n} \\ B_{1,n} \end{Bmatrix} \tag{8}$$

with $\zeta_{\alpha,n}(h) = (\frac{k-\nu_\alpha}{k_\alpha})^n e^{-\nu_\alpha h}$, and $\zeta_{\beta,n}(h) = (\frac{k-\nu_\beta}{k_\beta})^n e^{-\nu_\beta h}$.

The presence of both the underground tunnel and the half-space flat surface above will result in additional reflected waves generated (Equation (3)). They will now be expressed in integral form, with respect to the rectangular coordinate system *(x, y)* with origin *O* at the half-space surface, where for $y_1 \le h$ in the half-space, they take the form, with $x_1 = x,\ y_1 = y + h$:

$$\phi_2^s(x_1,y_1) = \int_{-\infty}^{\infty} [\mathbf{a_2}(k)]e^{ikx_1+\nu_\alpha y_1}e^{-\nu_\alpha h}\, dk \qquad \psi_2^s(x_1,y_1) = \int_{-\infty}^{\infty} [\mathbf{b_2}(k)]e^{ikx_1+\nu_\beta y_1}e^{-\nu_\beta h}\, dk \tag{9}$$

In other words, Equations (7) and (9) transform the scattered cylindrical waves in the half space from waves in cylindrical coordinates to that in rectangular coordinates, where the free-stress boundary conditions at the half-space surface, *y = 0*, are straight forward, comparatively, to be applied. Such detailed description of both the analytical process and their transformation back from rectangular to cylindrical coordinates, together with their numerical implementation, are given in Lin et al (2008) and will not be repeated here.

4. RESULTS AND DISCUSSIONS

A computer program in Visual Fortran to calculate the displacement amplitudes and phrases on nearby half-space surface above the tunnel was developed (Lin et al, 2008). A Poisson Ratio of $\nu = 0.25$ is also assumed unless otherwise specified. Following all previous work, it is convenient to express the frequency of the incident, reflected and scattered waves in terms of the dimensionless parameter η defined as follows (Trifunac,1973):

$$\eta = \frac{k_\beta a}{\pi} = \frac{\omega a}{\pi c_\beta} = \frac{2a}{c_\beta T} = \frac{2a}{\lambda} \tag{10}$$

Figure 2

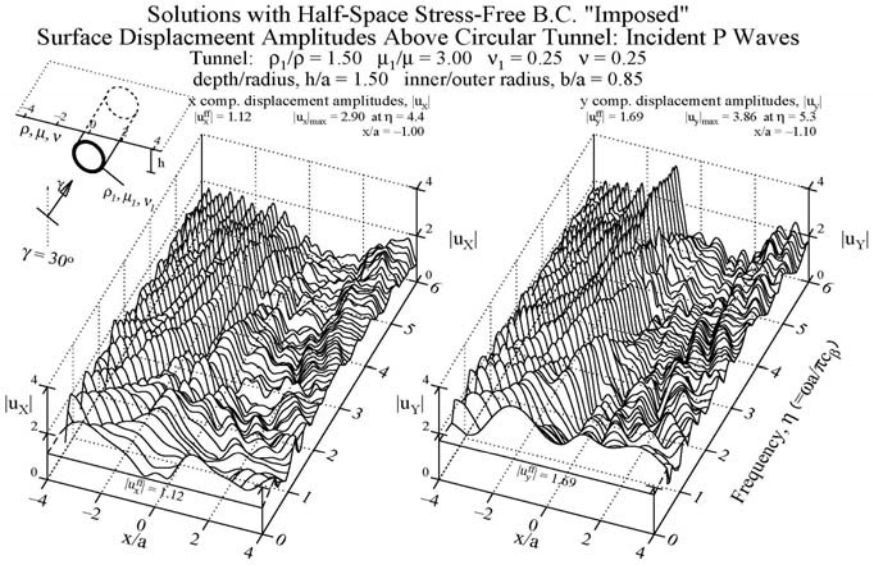

Figure 2 shows, the horizontal and vertical components of displacement amplitudes, $|u_x|$ and $|u_y|$, respectively along the surface of the half-space. They are 3D plots of displacement amplitudes plotted versus the dimensionless distance *x/a* and dimensionless frequency $\eta = \omega a / \pi c_\beta$.

In the figure, the plane P-waves have an incident angle of $\gamma = 30^o$ with respect to the vertical direction. The displacement amplitudes along the surfaces are plotted from $x/a = -4$ to $x/a = +4$, and for dimensionless frequency η in the range $0 < \eta \le 6$.

.The circular tunnel of outer radius a is at a distance of h below the surface with $h/a = 1.50$. The inner radius of the tunnel is b, with the ratio b/a = 0.85. The ratio of the mass densities of the tunnel to that of the half-space is $\rho_1 / \rho = 1.50$, and the ratio of their shear modulus is $\mu_1 / \mu = 3.00$, with the same Poisson ratio of $\upsilon = \upsilon_1 = 0.25$ for both the half space and tunnel medium. This makes the tunnel stiffer than the surrounding medium. In the absence of the underground tunnel, for a uniform half-space, the free-field amplitude of the ground displacement would be constant at $|u_x^{ff}| = 1.12$ and $|u_y^{ff}| = 1.69$ respectively in the x- and y- directions.

Lee and Cao (1989), Cao and Lee (1990), in their earlier work on wave diffractions around shallow circular canyons, observed that the incident P- waves at low frequency, with wavelength much longer than the topography in the displacement field, *"do not sense nor see"* the presence of the obstacle as much as the higher frequency (with shorter wavelength) incident P waves. The same observations were made by Lee and Karl (1992, 1993) for the same underground model studied here for incident P and SV waves. There the underground topography is a circular cavity. The same conclusion can be drawn from Figure 2 here for both the horizontal and vertical components, where at low frequencies, $0 < \eta << 1$, the displacement amplitudes deviate slightly from the free-field amplitudes (plotted at $\eta = 0$), but as the frequencies increase, the oscillations of the

amplitudes increase, together with the amplification of the amplitudes at each frequency getting higher and higher. For incident angle of $\gamma = 30^o$, a displacement amplitude close to 4 was observed at some frequency $\left(\max|u_x| = 3.86 \text{ at } \eta = 5.3\right)$, corresponding to an amplification of almost 2.

Previous works on the diffraction and scattering of anti-plane SH waves by surface and sub-surface topographies all observed a typical diffraction pattern for the SH waves, one that exhibit specific characteristics both in front of and behind the topography resulted from the diffraction of the incoming waves. The left and front sides of half-space exhibit standing waves pattern, while on the half-space surface to the right of the tunnel, with the tunnel acting as a barrier, a shadow zone is created, with waves of decreasing amplitudes that are also slightly smoother, quite a contrast to the standing wave pattern on the left side. The present and subsequent figures here show that the same wave pattern can also be observed for the in-plane P- and SV- waves. The only difference may be that the in-plane pattern is comparatively less significant here than of the SH wave cases. The in-plane waves also have two components of motions, and are further complicated by the presence of waves of both the longitudinal (P-) and transverse (SV-) mode types, so one of the two horizontal components can have a more significant pattern.

Figure 3

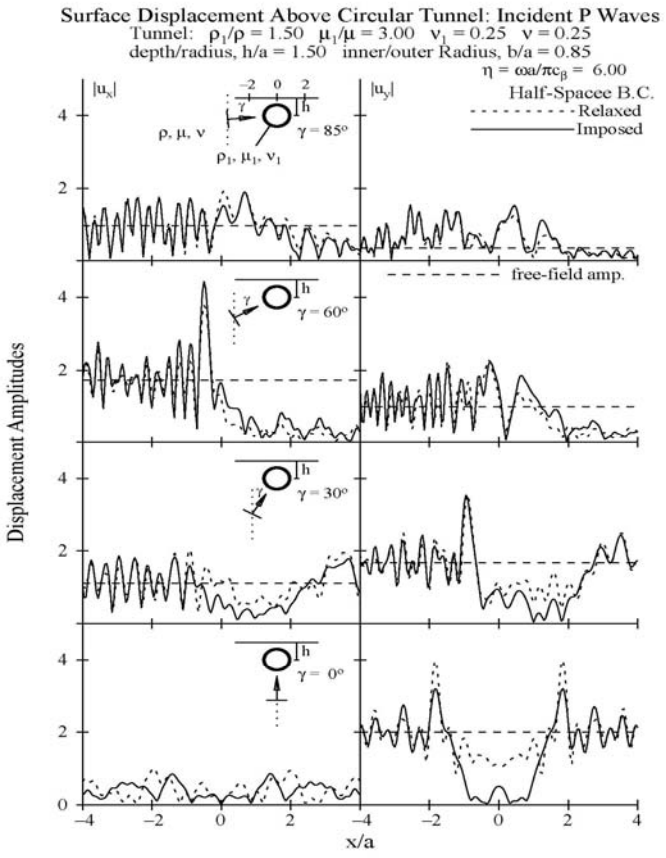

Figure 3 is a 2D plot of the displacement amplitudes at the half-space surface above the tunnel at 4 angles of incidence for both the x- and y- components of motions. All plots are at the same dimensionless frequency of $\eta = \omega a / \pi c_\beta = 6.00$. The same ratios of shear modulus, $\mu_1 / \mu = 3.00$, mass densities, $\rho_1 / \rho = 1.50$, and Poisson ratios, $\upsilon = \upsilon_1 = 0.25$, will be used as in previous plots. The same ratios of depth-to-radius ($h/a = 1.50$) and inner-to-outer radius (b/a = 0.85) are also used. The four angles of incidence, from bottom to top are respectively $\gamma = 0^o$ (veritcal), 30^o, 60^o and 85^o (almost horizontal) incidences. The left column plots are the horizontal x- component plots, while the right column plots are the vertical y-component plots. The graphs in each plot have the amplitudes in the y-axis versus the dimensionless coordinate *x/a* in the horizontal axis, in the range of [-4,4]. At each plot, the horizontal dashed line corresponds to the free-field displacement amplitude at the half-space surface in the absence of the underground tunnel.

Superimposed on this are the resultant amplitudes of the two types of waves, waves calculated with the half-space stress-free boundary conditions 1: "imposed" and 2: "relaxed" (free-field B.C. not applied). They are represented respectively by the wriggling solid lines and dashed lines and will be referred from here on as the "Imposed" waves and "Relaxed" waves. The two bottom plots for the x- and y- components are for $\gamma = 0^o$, the case of vertical incidence, which produces symmetric plots for both components of the "Imposed" (solid) waves and "Relaxed" (dashed) waves, as expected physically. Both the "Imposed" and "Relaxed" waves have very

similar wriggles, though the "Relaxed" waves do appear to have higher maximum amplitudes in the vertical y-component of motion, though both maxima occur at the same point of x/a on the half-space surface.. The maximum amplitude at the dimensionless frequency of $\eta = 6.00$, is around 3 for the "imposed" waves and is almost 4 for the "relaxed" waves. A displacement amplitude of 4 here, for a free-field amplitude of 2, thus corresponds to an amplification of 2. The next two sets of plots up above, the cases of $\gamma = 30^o$ and $\gamma = 60^o$, both show, for one of the components, the pattern of standing, oscillatory waves on the left versus shadowy, smoother waves on the right. This is more so for the y-component of the waves at $\gamma = 30^o$, and the x-component of the waves at $\gamma = 60^o$. As in the case of vertical incidence, both the "Imposed" and "Relaxed" waves have very similar wriggles, and their maximum amplitudes are much closer in location and amplitudes. For $\gamma = 60^o$, the maximum amplitude of the "Imposed" waves is over 4, while that of the "relaxed" waves is below but close to 4. The "Imposed" waves thus have an amplification of over 2. The top plots are for $\gamma = 85^o$, the case of almost horizontal incidence. It is not as interesting as the other three cases of incidences, as both the free-field and diffracted amplitudes of the waves are comparatively lower.

5. CONCLUSION

In summary, this paper illustrates the success of applying the flat half-space zero stress boundary conditions onto the cylindrical waves that are scattered and diffracted from surface and sub-surface circular topographies. It serve as a general method for more complicated wave propagation problems, like the diffraction problems involving surface and sub-surface topographies in a poroelastic half-space medium.

REFERENCES

H. Lamb (1904) On the Propagation of Tremors over the Surface of Elastic Solid, *Phil. Trans. Royal Soc. A203,* London, 1904.

V.R. Thiruvenkataher & K. Viswananthan (1965) Dynamic response of an Elastic Half Space with Cylindrical Cavity to Time Dependent Surface Tractions over the Boundary of the Cavity, *J. Math. Mech., 12* 541-571, 1965.

M.D. Trifunac (1973) A Note on Scattering of Plane SH Waves by a Semi-Cylindrical Canyon, *Int. J. of Earthquake Engineering and Struct. Dynamics,* 1, 267-281, pp.14, 1973.

V. W. Lee (1977) On Deformations Near Circular Underground Cavity Subjected to Incident Plane SH Waves, *Symposium of Applications of Computer Methods in Engineering, Aug* 23-26, 951-961, *Univ. of Southern California., Los Angeles, U.S.A.,,* 1977.

V.W. Lee & M.D. Trifunac (1979) Response of Tunnels to Incident SH Waves, *J. Eng. Mech., A.S.C.E.,*105, 643-659, *17 Pages, 4 Refs.,* Aug, 79.

V. W. Lee & H. Cao (1989) Diffraction of SV Waves by Circular Cylindrical Canyons of Various Depths, *J. Eng. Mech., A.S.C.E., 115(9),* 2035-2056, *22 Pages, 23 Refs.,* Sep, 89

H. Cao & V. W. Lee (1989) Scattering of Plane SH Waves by Circular Cylindrical Canyons with Variable Depth-to-Width Ratio, *European J. Earthquake Eng., III(2),* 29-37, *8 Pages, 10 Refs.,* Dec, 89.

H. Cao & V. W. Lee (1990) Scattering and Diffraction of Plane P Waves by Circular Cylindrical Canyons with Variable Depth-to-Width Ratio, *Int. J. Soil Dynamics & Earthquake Eng., 9(3),* 141-150, *10 Pages, 16 Refs.,* May, 90.

M.I. Todorovska & V. W. Lee (1990) A Note on Response of Shallow Circular Valleys to Rayleigh Waves: Analytical Approach, *Earthquake Eng. & Eng. Vibration, 10(1),* 21-34, Mar, 90

M.I. Todorovska & V. W. Lee (1991a) Surface Motion of Shallow Circular Alluvial Valleys for Incident Plane SH Waves -Analytical Solution, *Int. J. Soil Dynamics & Earthquake Eng., 10(4),* 192-200, *9 Pages, 30 Refs.,* May, 91

M.I. Todorovska & V. W. Lee (1991b) A Note on Scattering of Rayleigh Waves by Shallow Circular Canyons: Analytical Approach, ISET J. Earthquake Technology, *28(2),* 1-16 , *16 Pages, 15 Refs.,* Jun, 91.

V. W. Lee & J. Karl (1992) Diffraction of SV Waves by underground, Cicular, Cylindrical Cavities, *Int. J. Soil Dynamics & Earthquake Eng., 11(8),* (1992), 445-456, *12 Pages, 18 Refs.,* Jun, 92.

V. W. Lee & J. Karl (1993) Diffraction of Elastic Plane P Waves by Circular, Underground Unlined Tunnels, *European J. Earthquake Eng., VI(1),* 29-36, *8 Pages, 15 Refs.,* Aug, 93.
V. W. Lee & X.Y. Wu (1994a) Application of the Weighted Residual Method to Diffraction by 2-D Canyons of Arbitrary Shape, I: Incident SH Waves, *Int. J. Soil Dynamics & Earthquake Eng., 13(5),* 1994, 355-364, *10 Pages, 17 Refs.,* Oct, 94.
V. W. Lee & X.Y. Wu (1994b) Application of the Weighted Residual Method to Diffraction by 2-D Canyons of Arbitrary Shape, II: Incident P, SV & Rayleigh Waves, *Int. J. Soil Dynamics & Earthquake Eng., 13(5),* 1994, 365-373, *9 Pages, 24 Refs.,* Oct, 94.
V. W. Lee & M.E. Manoogian (1995) Surface Motion above an Arbitrary shape Underground Cavity for Incident SH Waves, *European J. Earthquake Eng., VII(1),* 3-11, *9 Pages, 13 Refs.,* Aug, 95.
A.J. Schiff (1995) Northridge Earthquake - Lifeline Performance and Post-Earthquake Response, Editor, *ASCE Technical Council on Lifeline Earthquake Engineering, Monograph No. 8,* 339 Pages, *ISBN 0784401063,* Aug, 95.
M.E. Manoogian & V. W. Lee (1996) Diffraction of SH-Waves by Subsurface Inclusions of Arbitrary Shape, *J. Eng. Mech., A.S.C.E., 122(2),* 123-129, *7 Pages, 15 Refs.,* Feb, 96.
M.D. Trifunac, M.I. Todorovska and V.W. Lee (1998) The Rinaldi Strong Motion Accelerogram of the Northridge, California, Earthquake of 17 January, 1994, *Earthquake Spectra*, *14(1), 225-239,* 1998.
V. W. Lee, S. Chen & LR. Hsu (1999) Antiplane Diffraction from Canyon Above a Subsurface Unlined Tunnel, *J. Eng. Mech., A.S.C.E., 125(6),* 668-675, *8 Pages, 24 Refs.,* Jun, 99.
M.E. Manoogian & V. W. Lee (1999) Antiplane Deformations Near Arbitrary-Shape Alluvial Valleys, *ISET J. Earthquake Technology, 36(2), 107-120, 14 Pages, 63 Refs.,* Jun, 99.
J. Liang, Y. Zhang, X Gu & V. W. Lee (2000) Surface Motion of Circular-Arc Layered Alluvial Valley for Incident Plane SH Waves, Chinese *J. Geotechnical Engineering, 22(4),* 396-401, *6 Pages, 12 Refs.,* Jul, 00.
J. Liang, H. Zhang & V.W. Lee (2001) Scattering of Plane P Waves around Circular-Arc Layered Alluvial Valleys: Analytical Solution, *ACTA Seismologica Sinica 14(2), 176-195, 20 Pages, 9 Refs.,* Mar, 01.
C.A. Davis, V. W. Lee & J.P. Bardet (2001) Transverse Response of Underground Cavities and Pipes to Incident SV Waves, *Int. J. Earthquake Eng. & Structural Dynamics, 30(3),* 383-410, *18 Pages, 26 Refs.,* Feb, 01.
J. Liang, L. Yan & V.W. Lee (2001) Effect of a Covering Layer in a Circular-Arc Canyon on Incident Plane SV Waves, [pdf]?? *ACTA Seismologica Sinica 14(6) 660-675, 16 Pages, 9 Refs.,* Nov, 01.
V.W. Lee, M.E. Monoogion & S. Chen (2002) Antiplane Deformations Near a Surface Rigid Foundation Above a Subsurface Rigid Circular Tunnel, *Int. J. Earthquake Eng. & Eng. Vibration, 1(1),* Jun, 02.
J. Liang, L. Yan & V. W. Lee (2002) Scattering of Incident Plane P Waves by a Circular-Arc Canyon with a Covering Layer, *ACTA Mechanica Solida Sinica,23(4),* Dec, 02.
N. Dermendjian, V.W. Lee & J-W. Liang (2003) Anti-plane Deformations around Arbitrary-Shaped Canyons on a Wedge-Shaped Half-Space: Moment Method Solutions, *Int. J. Earthquake Eng. & Eng. Vibration, 2(2) 281-288, 2003.*
J. Liang, Y. Zhang, X Gu & V. W. Lee (2003) Scattering of Plane Elastic SH Waves by Circular-Arc Layered Canyons, *Journal of Engineering Vibrations, 16(2) 158-165,* 2003.
J.W. Liang, H. Zhang & V.W. Lee (2003) A Series Solution for Surface Motion Amplification due to Underground Twin Tunnels: Incident SV Waves, *Int. J. Earthquake Eng. & Eng. Vibration, 2(2) 289-298,* 03.
N. Dermendjian & V. W. Lee (2003) Moment Solutions of Anti-Plane (SH) Diffraction Around Arbitrary-Shaped Rigid Foundations On a Wedge-Shape Half Space, *ISET J. Earthquake Technology, 40(4) 161-172,* Dec, 03.
J. Liang, H. Zhang & V.W. Lee (2004) A Series Solution for Surface Motion Amplification due to Underground Group Cavities: Incident P Waves, *ACTA Seismologica Sinica 17(3) 296-307,* May, 04.
J. Liang, H. Zhang & V.W. Lee (2004) An analytical solution for dynamic stress concentration of underground twin cavities due to incident SV waves , *Journal of Vibration Engineering 17(2) 132-140* Jun 04.
J. Liang, H. Zhang & V.W. Lee (2004) An analytical solution for dynamic stress concentration of underground cavities under incident P waves, *Journal of Geotechnical Engineering 26(6) 815-819* Nov 04.
J. Liang, Z. Ba & V.W. Lee (2006) Diffraction of SV Waves by a Shallow Circular-arc Canyon in a Saturated Poroelastic Half-Space, *Spec. issue Honoring Biot, Int.* J. *Soil Dynamics & Earthquake Eng.,26(6-7) 582-610*, *(Special issue on Biot Centennial – Earthquake Engineering,*. Jun-Jul, 06.
Todorovska, M.I. & Y. Al Rjoub (2006) Plain strain soil-structure interaction model for a building supported by a circular foundation embedded in a poroelastic half-space, *Soil Dynamics and Earthquake Engrg, 26(6-7), 694-707. (Special issue on Biot Centennial – Earthquake Engineering),* Jun-Jul, 06.
C.H. Lin, V.W. Lee M.I. Todorovska & M.D. Trifunac (2008) Zero-Stress Cylindrical Wave Functions Around a Circular Underground Tunnel in a Flat Elastic Half-Space: Incident P Waves, (to be submitted for publication).